Catalysis Science & Technology

PAPER

View Article Online
View Journal

Cite this: DOI: 10.1039/c4cy00990h

Catalytic performance of a novel Cr/ZnAlLaO catalyst for oxidative dehydrogenation of isobutane

Li He,*[a] Li Fu[b] and Yingzhan Tang[c]

Received 1st August 2014,
Accepted 23rd September 2014

DOI: 10.1039/c4cy00990h

www.rsc.org/catalysis

The oxidative dehydrogenation of isobutane using a chrome-based catalyst supported on a novel ZnAlLaO mixed oxide was investigated. The characterization and performance of Cr/ZnAlLaO catalysts were compared with those of several traditional catalysts. The Cr/ZnAlLaO catalyst showed the best selectivity and conversion rate with the highest stability. The performance of the Cr/ZnAlLaO catalyst strongly depends on the Cr content and support properties. The activity peak of isobutane oxidative dehydrogenation occurs at 18 wt% of Cr_2O_3 loading. The selectivity and conversion of isobutene reach their maximum at 84.07% and 52.44%, respectively. Correlation was observed between coke formation and catalyst deactivation. Moderate alkalinity on the ZnAlLaO support surface is helpful to suppress coke formation as well as to improve the catalytic activity and stability. Appropriate water vapour addition to the feed can improve catalytic stability, while both the selectivity of isobutene and the conversion of isobutane decreased.

Introduction

In recent years, the oxidative dehydrogenation (ODH) of isobutane has received considerable research attention as a route to obtain isobutene (an additive of petrol used for replacing lead-containing compounds).[1] Due to the development of the petroleum and chemical industries, many green technologies were developed for using alkanes. Isobutene is an intermediate mainly from catalytic cracking of petroleum by-products. Chromium supported on alumina was widely employed in this reaction as a catalyst. However, it also exhibits several undesired features such as catalysing side reactions like coking and cracking, finally leading to catalyst deactivation.[2] Most of these disadvantages could be avoided by improving the properties of the catalyst. Hence, the most important challenge is to develop a more effective catalytic system which could produce a high yield of the required isobutene products. Supported chromium oxide-based catalysts have been studied for many decades as an active component in many reactions, one of which is the ODH of isobutane to isobutene. Jibril *et al.*[3] studied the chromium oxide-based catalytic activity on different support surfaces. The result showed that the order of isobutane conversion rate under 250 °C is as follows: Cr_2O_3/Al_2O_3 (11.0%) > Cr_2O_3/SiO_2 (8.4%) ≈ Cr_2O_3/TiO_2 (8.2%) > Cr_2O_3/MgO (7.1%). Sloczynski *et al.*[4] studied the chrome activities on different supports with the following sequence: $Al_2O_3 \approx ZrO_2 > MgO > TiO_2 > SiO_2$. Recently, studies demonstrated that the chromium oxide-based catalysts used for the ODH of isobutane on different supports could be activated at relatively low temperatures, 200–300 °C.[5,6] According to the different systems, the maximum selectivity of isobutene was between 50% and 80% and the conversion of isobutene was about 10–20%. The Al_2O_3 catalysts exhibit the best performance among these catalysts. However, the action stability and the activity of the catalysts are still not satisfactory. Thus, it is necessary to further improve the catalytic performance of Al_2O_3 catalysts in the ODH of isobutane.

Recently, numerous studies have been carried out to measure the modification of the stability and activity of Al_2O_3 catalysts by adding some alkali metals as active components, such as Pt, Cr, Sn and Ni. Systems with relatively low Cr surface concentration and chromium oxide-based catalysts with higher concentrations of Cr applied in industrial plants, generally supported on alumina with alkali oxides as promoters, were compared.[7] After addition of the Cr active component and the additive K_2O, $K–CrO_X/Al_2O_3$, the catalyst exhibited the best performance. McVicker *et al.*[8] reported the relationship between the acidity and the basicity on the support surface as well as the relationship between catalytic reaction performance and resistance to carbon deposition. Moreover, a further attraction of the ODH of isobutane is the modification of supports with elements such as Zn and La.[9]

In the present study, various chrome-based catalyst supports and a Cr/ZnAlLaO catalyst with different Cr contents

[a] Beijing Petrochemical Engineering Corp. LTD, Chaoyang District Tianjuyuan Building No. 7, Beijing, China. E-mail: heli_0619@163.com
[b] Department of Chemistry and Biotechnology, Faculty of Science, Engineering and Technology, Swinburne University of Technology, Hawthorn VIC 3122, Australia
[c] Shenzhen institute, Hong Kong City of University of Research Centre, Nanshan District Yuexing 2 Way No. 8, China

were prepared for the dehydrogenation of isobutane. The objective was to study the catalytic and chemical–physical properties in the ODH of isobutane. Cr/ZnAlLaO catalysts with different amounts of Cr loading were investigated by several techniques, including XRD, CO_2-TPD and XPS. The reaction conditions such as reaction temperature, alkoxy oxygen ratio and the influence of water vapour were optimized in detail. The catalytic performance was carried out at a relatively lower temperature than that applied industrially. All the results obtained are compared with literature data in an effort to provide important information and form a better understanding of the Cr/ZnAlLaO catalyst on this catalytic system of ODH.

Experimental

Catalyst preparation

Catalysts were prepared according to the procedure described as follows.[10] Pseudo-boehmite (AlOOH) powder was originally calcined at 600 °C for 3 h in order to obtain γ-Al_2O_3. Appropriate amounts of γ-Al_2O_3 with $Zn(NO_3)_2{\cdot}6H_2O$ (Al/Zn = 8.5–10.5, molar ratio) and $La(NO_3)_3{\cdot}6H_2O$ (La/Al = 0.025, molar ratio) were mixed evenly, and then an appropriate amount of diluted nitric acid aqueous solution (AR, 99%) (2 wt.%) as an adhesive solvent was added dropwise until the powder mixture bonded together evenly to form a dough. Then, it was extruded *via* a banded extruder (using an extrusion moulding method) to form original supports. After drying in a stoving chest at 50 °C for 12 hours, the supports were cut into cylindrical particles with lengths of about 2 mm to 3 mm. Finally, the cylindrical supports were calcined in a muffle furnace at 650 °C for 5 hours.

Subsequently, Cr was introduced into calcined ZnAlLaO by immersing the ZnAlLaO support in different concentrations of $Cr(NO_3)_3{\cdot}9H_2O$ aqueous solution. Typically, the support was first immersed in the prepared $Cr(NO_3)_3{\cdot}9H_2O$ solution for about 15 min in a stirred vessel with the temperature maintained at 60 °C. After drying in a stoving chest at 105 °C for 12 h, the dried catalyst was calcined at 500 °C for 4 h with steam for dechlorination. The heating rate was 2 °C min^{-1}. Then the catalyst was heated to 700 °C and maintained at this temperature for a further 5 h.

Catalyst testing

The catalytic activity measurements were carried out in a continuous-flow reaction system consisting of stainless steel single-pipe fixed-bed reactors (Φ = 9 × 2 mm, 500 mm in length) with a gas chromatograph for online product analysis. 2 g of catalysts were used each time. The reactant gases were fed through the mass flow controllers (MFC), which were used to deliver a defined flow of each gas. The ratio of i-C_4H_{10}/O_2 was 3.5 (molar ratio) at a space velocity (SV) of 200 mL g^{-1} h^{-1}. The feed composition was obtained by mixing 6.67 mL min^{-1} of isobutane, 1.67 mL min^{-1} of oxygen and 0.05 mL min^{-1} of water vapour under normal conditions. For the tests without water vapour, the feed composition was calculated by keeping the same ratio of i-C_4H_{10}/O_2 and SV. The activity measurements were carried out at 560–600 °C under atmospheric pressure. The reaction temperature was measured with three thermocouples, one at the top, one at the middle, and another at the bottom, placed near the catalyst bed, and was maintained constant at 580 °C for 10 h under normal conditions. Fig. 1 displays the flow diagram of the ODH.

Reactants and products were analysed online using gas chromatography, and products were analysed online using a gas chromatograph–mass spectrometer (SP2100) equipped with three sample loops and a 13-port sampling valve. One sample loop was injected into an alumina PLOT column, and then eluting products were detected with a flame ionization detector (FID). The second sample loop was injected into a second alumina PLOT column (Φ = 1/8 in × 3 m) and analysed by mass spectrometry. The contents of the third sample loop were injected into a Hayesep N column (Φ = 1/8 in × 2 m) used to adsorb CO_2, H_2O and heavy hydrocarbons connected in series with a Molecular Sieve 5A packed column. The products eluting from this column were detected with a thermal conductivity detector (TCD). The analytical conditions were as follows: carrier gas, nitrogen; column temperature, 50 °C; temperature of the TCD detector, 100 °C; sample amount, 5 μL. The catalyst behaviour was evaluated according to the formulas given below.

Conversation of isobutane:

$$X_{\text{isobutane}} = \frac{F_{\text{isobutane, in}} - F_{\text{isobutane, out}}}{F_{\text{isobutane, in}}}$$

Selectivity of isobutene:

$$S_{\text{isobutane}} = \frac{F_{\text{isobutane}}}{F_{\text{isobutane, in}} - F_{\text{isobutane, out}}}$$

where F is the molar flow rate.

X-ray diffraction (XRD) of the catalysts was performed using a D8 Advance (Bruker, Germany) instrument with Cu Kα radiation (40 kV and 30 mA). XRD data were collected in the 2θ range of 10° to 90° using a scan speed of 12° min^{-1} and a step size of 0.02°.

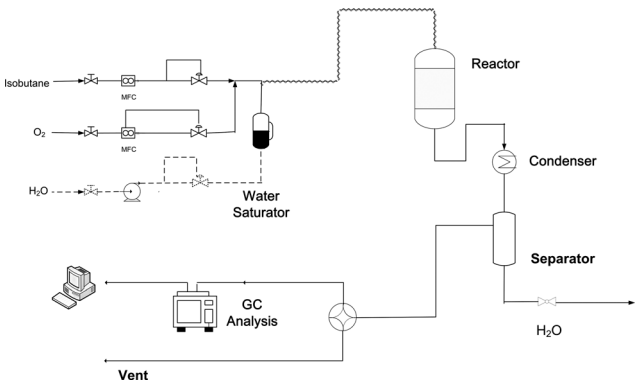

Fig. 1 Flow diagram of the dehydrogenation of isobutene.

Temperature-programmed desorption (TPD) characterization of the catalysts was performed with a quadrupole mass spectrometer (AMETEK HQ 200 M, USA) in a quartz fixed-bed reactor with an inner diameter of 6 mm. Catalysts (0.4 g) were placed in the TPD reactor and reduced under 10% (v/v) H_2/Ar flow at 600 °C for 0.5 h. Then the temperature was dropped to 400 °C for 10 min and the reactor was purged with Ar gas (30 mL min^{-1}) to remove the H_2 and steam. After naturally cooling down to room temperature, the temperature of the reactor was adjusted by a cooling machine. CO_2 or isobutene was adsorbed on the catalyst at −5 to −8 °C for 1 h. After the reactor was purged under Ar flow (30 mL min^{-1}) for 1 h, the adsorbate was desorbed by heating at 15 °C min^{-1} under Ar flow.

X-ray photoelectron spectroscopy (XPS) measurements were performed with an Axis Ultra DLD (a delay-line detector) spectrometer (ThermoScientific, USA) using a focused monochromatized AlKα radiation (1486.6 eV) in the CAE mode. The material was introduced into the treatment chamber using double-sided tape. The sample was maintained under high vacuum at 5.0×10^{-9} mbar. It was reported that the high-resolution XPS region scan spectra were obtained within a short period (*ca.* 12 min) at 20 eV pass energy to minimize the photo-reduction of the surface chromium species that may be induced by X-rays.[11–13] The composition of different chemical states of surface chromium in the samples was obtained from XPS spectra using Vision 2.0 software.

Results and discussion

XRD and CO_2-TPD characterization of different support catalysts

Fig. 3 shows the XRD patterns of the same Cr active component on different types of supports. The diffraction peaks of different supports indicate that the Cr in the samples is a partially amorphous phase or a small crystalline particle due to the difficulties in interaction between Cr with TiO_2 and SiO_2.[14] As shown in the XRD patterns of both Cr/TiO_2 and Cr/SiO_2, it can be deduced that the bulk Cr_2O_3 gathered on the support surface and the active component was dispersed unevenly. In Fig. 2, it can be seen from the pictures that the active component Cr over the CaAlLaO support is caked on the external surface, indicating uneven dispersity. The Cr on the CaAlLaO catalyst showed agglomeration; the active component cannot be fully utilized on the surface. For the CrAlLaO catalyst, due to the self-containing property of the Cr element, the CrAlLaO interacted with the active component and exhibited strong *syn*-Cr_2O_3 diffraction peaks. It can be

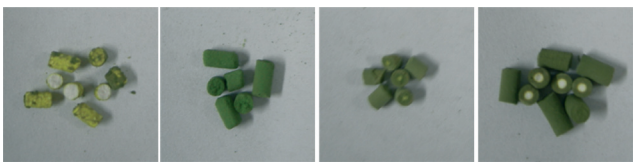

Fig. 2 Pictures of different supports used for loading Cr. (a) Cr/CaAlLaO, (b) Cr/CrAlLaO, (c) Cr/MgAlLaO, and (d) Cr/ZnAlLaO. Cr loading: 18 wt%.

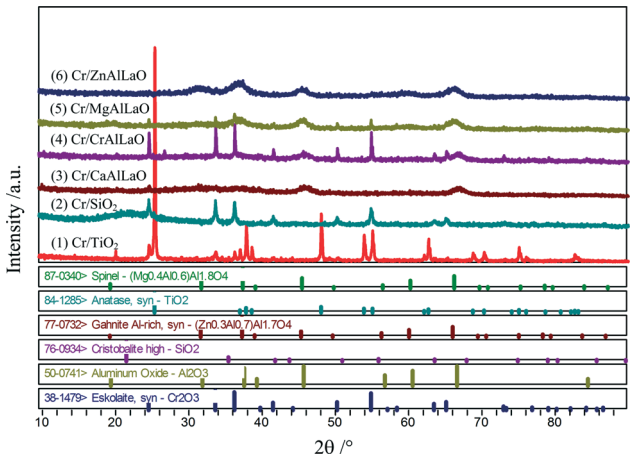

Fig. 3 XRD patterns of different types of supports.

observed that the active component not only existed on the external surface of the catalyst but also penetrated into the interior. Hence, the utilization rate of the Cr active component on the catalyst's external surface should be lower than those of the MgAlLaO and ZnAlLaO catalysts. The reaction performance of various catalysts also proved this speculation (Fig. 4). As shown in the XRD pattern of the MgAlLaO catalyst, the magnesium aluminate spinel structure has been formed on the catalyst surface. The peaks at 37.904°, 46.102° and 67.275° can be indexed as $(Mg_{0.4}Al_{0.6})Al_{1.8}O_4$. The XRD pattern of the ZnAlLaO catalyst also shows that the diffraction peaks are assigned to the zinc–aluminum spinel phase $(Zn_{0.3}Al_{0.7})Al_{1.7}O_4$, which are slightly stronger than the diffraction peaks of MgAlLaO. It is probably due to the stronger interaction of the active component Cr with the ZnAlLaO support than that with the MgAlLaO support, which further enhances the diffraction peak intensity of Al_2O_3. Furthermore, no obvious diffraction peaks of Cr_2O_3 were observed for both Cr/MgAlLaO and Cr/ZnAlLaO catalysts. This implies that the active component dispersed evenly on the support surface. However, in Fig. 2, it can be seen clearly that the penetrated thickness of the active component in the ZnAlLaO catalyst is lower than that in the MgAlLaO catalyst. The active component of the ZnAlLaO

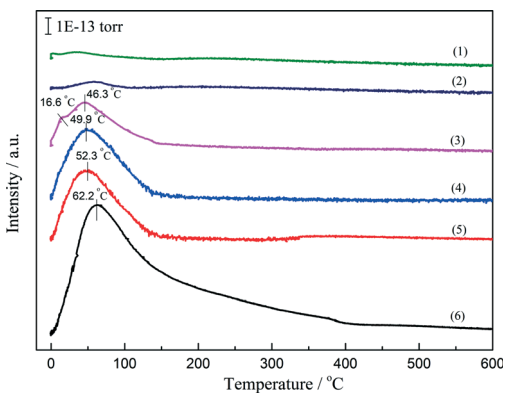

Fig. 4 CO_2-TPD profile of different supports: (1) TiO_2, (2) SiO_2, (3) Cr/ZnAlLaO, (4) Cr/MgAlLaO, (5) Cr/CrAlLaO, and (6) Cr/CaAlLaO.

catalyst is mainly distributed on the external surface, suggesting that the Cr utilization rate of the ZnAlLaO catalyst on the outside layer is higher than that of the MgAlLaO catalyst.[15,16]

In order to further study the influence of different supports on catalytic properties, CO_2-TPD experiments were carried out. Fig. 4 shows the CO_2-TPD profiles of the different samples. It can be observed that for SiO_2 and TiO_2 catalysts, there are no obvious desorption peaks observed, indicating almost no alkalinity on the support surfaces of SiO_2 and TiO_2. The CO_2-TPD profile of the CaAlLaO support shows the highest intensity with a desorption temperature of 62.2 °C. However, the CO_2 desorption peak areas of CrAlLaO, MgAlLaO and ZnAlLaO supports are relatively smaller than that of the CaAlLaO support, which indicates that these three supports have weaker alkalinity than that on the CaAlLaO support surface. Moreover, from the ZnAlLaO support emerged two CO_2 desorption peaks. The first peak located at 16.6 °C is assigned to the weak physical desorption peak. Another peak is the weak alkaline desorption centre that appeared at a temperature of 46.3 °C.

Generally, appropriate alkaline sites can significantly improve the catalytic ability of carbon elimination as well as enhance the catalytic stability.[17,18] The acidic sites are carbon ion activation centres, and these easily lead to catalyst carbon deposition. This is an important factor that causes the decrease in catalytic activity and stability. Thus, the appropriate alkalinity on the catalyst surface can improve the selectivity of isobutene and the resistance to carbon deposition. Weak acid sites adsorb isobutene easily and then form tertiary carbonium ions. Then the intermediates leave the catalyst surface to produce isobutene products.[19,20] If the isobutane is adsorbed on the acid sites, its intermediates cannot undergo desorption of the catalyst surface in a timely manner or immediately undergo adsorption again after desorption. This process could lead to deep oxidation of isobutane and then induce carbon deposition. The carbon deposition can cause catalyst deactivation and can decrease the selectivity of isobutene.[21] However, the alkaline centre can activate the oxygen element effectively on the ZnAlLaO support surface, promoting ODH reaction. We believe that the selectivity is associated with the lattice oxygen of the catalyst surface. The number of lattice oxygen atoms can improve the conversion rate of the catalyst and reduce its selectivity.[22,23] In addition, when the deep oxidation occurred on the catalyst surface and induced carbon deposition, the adjacent weak alkalinity site can activate the oxygen of the ZnAlLaO support and carbon deposition can be eliminated, consequently improving the stability and activity of the Cr/ZnAlLaO catalysts. It has also been proven, as shown in Fig. 4, that the selectivity and conversion rate of the ZnAlLaO catalyst are much higher than that of other catalysts. Therefore, we believe that moderate alkalinity and acidity are important factors for catalytic activity and stability.

Catalytic performance of different support catalysts

The catalytic performances of the different support catalysts are presented in Fig. 5. All catalysts showed decreasing catalytic activity along with the reaction time. The initial selectivities of isobutene catalyzed by Cr (18%)/MgAlLaO and Cr (18%)/ZnAlLaO are 78.87% and 84.07%, respectively. In our experiments, the Cr (18%)/ZnAlLaO catalyst exhibits the best catalytic performance and the highest selectivity conversion compared with the other five catalysts. This result is superior to that of previously reported 10% Cr/Al_2O_3 catalyst (63.1%) selectivity and 10.7% conversion when using $Cr(NO_3)_3{\cdot}9H_2O$ as a precursor, and 100% selectivity and 0.1% conversion when using $CrK(SO_4)_2{\cdot}12H_2O$ as a precursor. However, the Cr (18%)/ZnAlLaO catalyst also showed relatively unsatisfactory stability after 6 h of reaction.

In order to obtain better catalytic performance, we further studied the influence of the Cr content and water vapour.

XRD and CO_2-TPD characterization of different loadings on the ZnAlLaO catalyst

Several studies have proved that the addition of Cr to the ZnAlLaO catalyst could enhance the catalytic performance and the reaction stability.[24] The loading amount of Cr in this case acts as a promoter in ODH. As the loading amount of

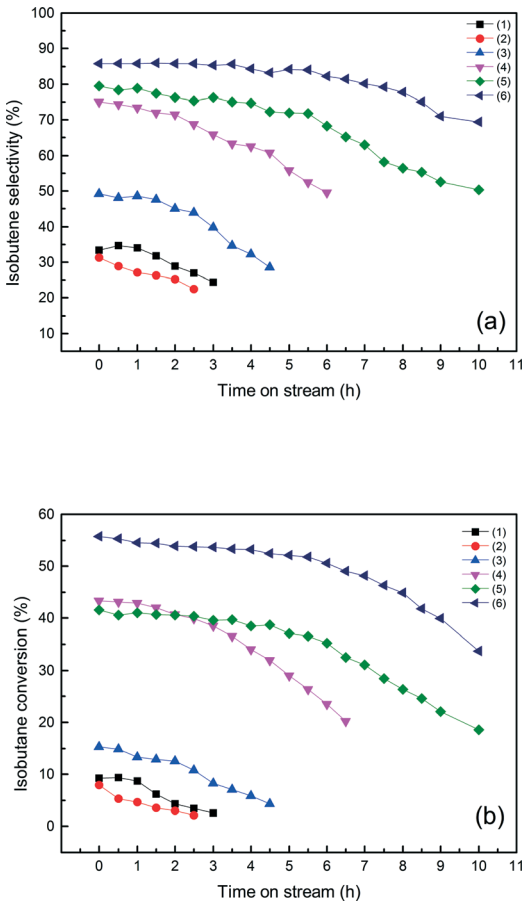

Fig. 5 (a) Selectivity and (b) conversion as functions of time for the different support catalysts: (1) Cr (18%)/TiO_2, (2) Cr (18%)/SiO_2, (3) Cr (18%)/CaAlLaO, (4) Cr (18%)/CrAlLaO, (5) Cr (18%)/MgAlLaO, and (6) Cr (18%)/ZnAlLaO. Reaction conditions: temperature = 580 °C, 1 atm, 2 g of catalysts, i-C_4H_{10}/O_2 = 3.5 (molar ratio), SV = 200 mL g^{-1} h^{-1}.

the active component Cr increases, the loading thickness on the external surface is also increased, which can be easily observed on the digital pictures (Fig. 6). In Fig. 5, the samples with Cr loadings of 8.56% and 18.12% did not obviously appear in the diffraction peaks associated with the Cr_2O_3 crystalline structure. The results suggest that Cr_2O_3 is highly dispersed in the loading range of 8% to 18%. The XRD patterns of the 8.56% and 18.12% Cr loadings show the appearance of the $(Zn_{0.3}Al_{0.7})Al_{1.7}O_4$ aluminium-rich zinc spinel lattice structure. It has been reported that Cr can diffuse into the oxygen vacancies in the $ZnAl_2O_4$ spinel lattice.[25] It can be observed that the $(Zn_{0.3}Al_{0.7})Al_{1.7}O_4$ spinel structure of the Cr (32.03%)/ZnAlLaO catalyst is damaged by the loading amount of Cr up to 32% on the catalyst surface. The diffraction peaks of Cr_2O_3 are significantly strengthened as well as the appearance of the Cr_2O_3 crystalline phase on the catalyst surface.

Fig. 8 shows the CO_2-TPD profiles of the different Cr loading samples. Generally, various catalysts appear in the CO_2 weak alkalinity peak range of 48 °C to 62 °C; low-temperature desorption peaks are assigned to CO_2 on Cr_2O_3.[26] It can be observed that the ZnAlLaO catalyst without active component Cr loading showed the strongest alkalinity compared with other catalysts. However, the ZnAlLaO catalyst without the active component has the lowest active performance. Consequently, higher alkalinity has disadvantages for the ODH reaction. As the active component Cr loading increases, the area of the CO_2 desorption peak decreases. The addition of Cr can lead to the formation of weak alkaline sites. In addition, the weak alkaline sites can effectively activate the oxygen element in the ZnAlLaO support,[26] inhibiting the production of coke. However the overloading of Cr results in the blocking effect of a worse Cr particle distribution on the catalyst surface, which has been proven from the XRD pattern in Fig. 7.

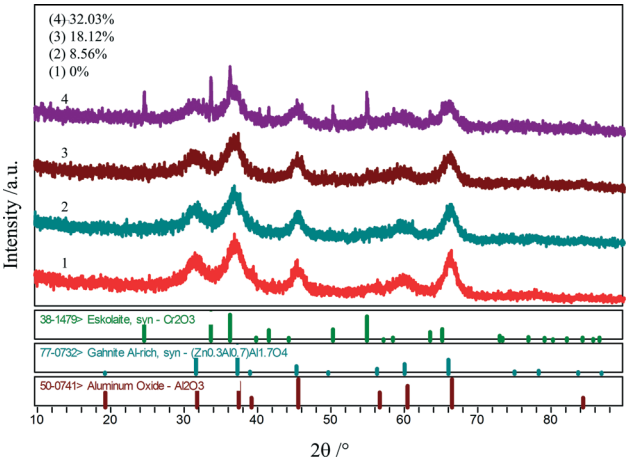

Fig. 7 XRD patterns of the catalysts with different Cr additions.

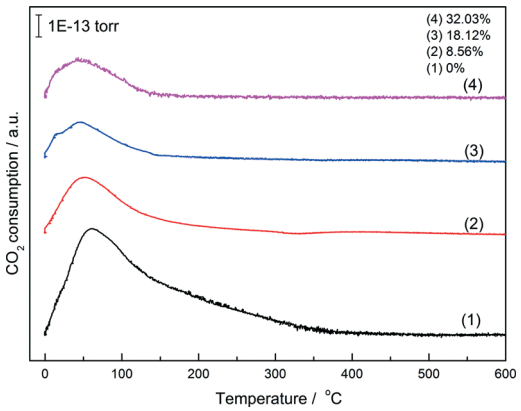

Fig. 8 CO_2-TPD profile of the catalysts with different Cr loadings. (1) Cr (0%)/ZnAlLaO, (2) Cr (8.56%)/ZnAlLaO, (3) Cr (18.12%)/ZnAlLaO, and (4) Cr (32.03%)/ZnAlLaO.

Catalytic performance of different Cr loadings on the ZnAlLaO catalyst

Fig. 9 shows the effect of the Cr content on the catalytic performance of the isobutane ODH over 10 h. The Cr (18.12%)/ZnAlLaO catalyst achieves the maximum isobutene selectivity (84.07% after reaction for 6 h). It has been studied that Cr has become a key ingredient in oxidative dehydrogenation catalysts because of its high activity for Cr–O–Al bond formation.[25] This is the reason for an intrinsic high selectivity of unprompted Cr toward isobutene ODH. On the other hand, it has been proven from the XRD pattern (Fig. 7) that these results obtained at a better performance level confirm the increase in dehydrogenation activity partly due to a better particle distribution prompted by suitable loading of Cr on the ZnAlLaO catalyst. However, the continuous addition of Cr leads to the decrease in catalytic activity due to the blocking effect of a worse Cr particle distribution on the catalyst surface.[27] The reactant gas can easily interact with the active sites due to overloading of Cr species and thus enhances uneven active component dispersion on the catalyst surface. This behaviour causes the occurrence of side reactions during this process and then leads to the decrease in the selectivity eventually. Hence, the active component disperses evenly and appropriate Cr loading (about 18%) on the catalyst surface is the reason for the enhancement of the catalytic activity and stability.

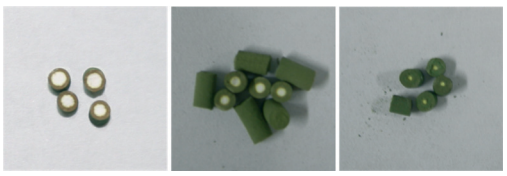

Fig. 6 Pictures of different supports used for loading Cr. (1) Cr (8.56%)/ZaAlLaO, (2) Cr (18.12%)/ZnAlLaO, and (3) Cr (32.03%)/ZnAlLaO.

According to the literature,[28,29] the formation of CO_X and CH_X species from readsorption of isobutane and isobutene is one of the significant factors for coke deposition on the catalyst surface; in this case, the carbon deposition on the catalyst surface may act as a reason to decrease the catalytic activity by deactivating the active sites.[30,31] Therefore,

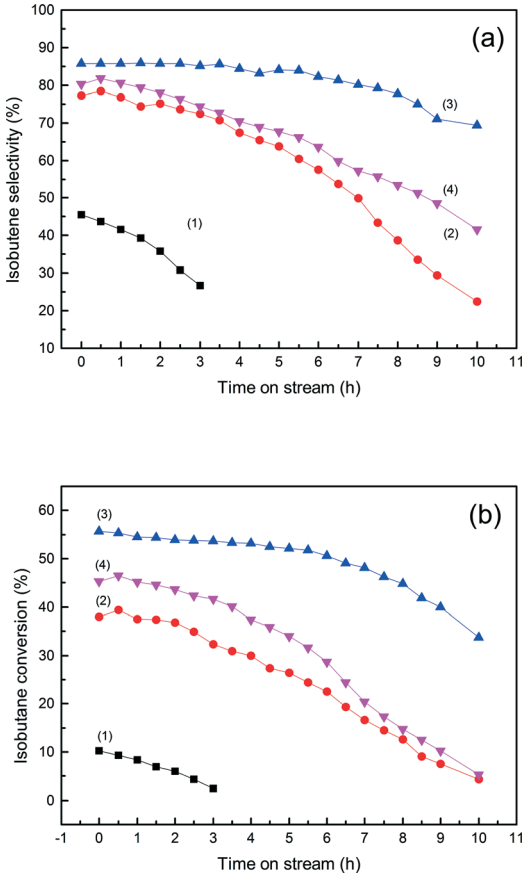

Fig. 9 (a) Selectivity and (b) conversion as functions of time for the different loading catalysts: (1) Cr (0%)/ZnAlLaO, (2) Cr (8.56%)/ZnAlLaO, (3) Cr (18.12%)/ZnAlLaO, and (4) Cr (32.03%)/ZnAlLaO. Reaction conditions: Al/Zn = 8.5–10.5, temperature = 580 °C, 1 atm, 2 g of catalysts, i-C_4H_{10}/O_2 = 3.5 (molar ratio), SV = 200 mL g^{-1} h^{-1}.

minimizing the readsorption and the dissociation of the C–C bond will effectively eliminate carbon deposition on the catalyst surface.[32] Subsequently, we did some experiments on the addition of water vapour and its influence as part of the feed gas for ODH.

The effects of water vapour

Water vapour is used as a diluent and oxidant in many dehydrogenation reactions in order to eliminate carbon deposition.[33,34] However, few studies have been reported on the use of water vapour as a feed gas for ODH reaction. Fig. 10 shows the 100 h reaction of the Cr/ZnAlLaO catalyst with steam as a diluent; it can be observed that the conversion of isobutene decreased significantly (32.74%) after 6 h, and CO_2 selectivity (10.92%) obviously increased after addition of water vapour. Without water vapour, small amounts of dehydrogenation products, such as unsaturated olefin, would be polymerized on a strong acid centre of the catalyst surface. Then, deep dehydrogenation would occur and eventually result in the formation of carbon deposit precursors. The water vapour could act as a diluent to reduce the partial pressure of oxygen in

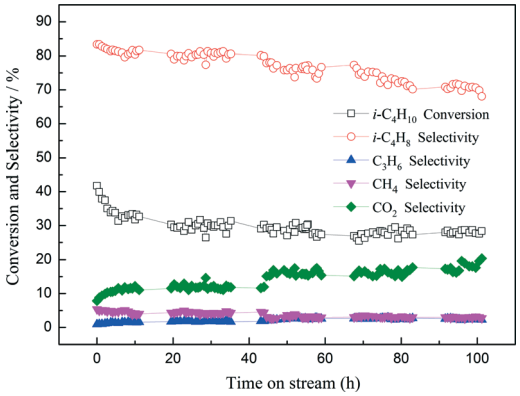

Fig. 10 100 h test of the Cr (18%)/ZnAlLaO catalyst with steam as a diluent. Reaction conditions: temperature = 580 °C, 1 atm, 2 g of catalysts, i-C_4H_{10}/O_2 = 3.5 (molar ratio), SV = 200 mL g^{-1} h^{-1}.

the reaction gas and promote the ODH reaction equilibrium towards the right. On the other hand, water vapour is responsible for reducing the acidity of the support surface and interacts with some carbon deposits to induce carbon deposit gasification. Thus, the CO_2 selectivity increased and side reactions occurred, such as steam reforming. It can also delay the coverage rate of carbon formation on the catalyst surface.[35] Due to adsorption of water molecules on the Cr_2O_3 surface, the adsorption and desorption capacity of oxygen species are decreased on the support surface. The interaction between the active component and the support can be weakened gradually.[36] Therefore, the addition of an appropriate amount of water vapour to the feed can continuously enhance the catalytic stability, while both the isobutane conversion and the isobutene selectivity decreased at the same time.

XPS analysis

Fig. 12(a) shows the XPS spectra in the Cr 2p region for various catalysts. The quantitative data of binding energies are illustrated in Table 1. Curve fitting of the experimental data showed the presence of two distinct chromium species. The oxidation states of the species have been totally assigned to Cr(III) and Cr(VI) at the binding peaks of 577 and 579 eV, respectively. It has been reported in ref. 37 that the oxidation states of chromium were determined by the binding energy of the Cr 2p(3/2) peak and the value of spin–orbit splitting Cr 2p(1/2)–Cr 2p(3/2). The binding energy decreases in the range of 576.4 eV to 576.9 eV for Cr(III). Due to the intrinsic

Table 1 Curve-fitting parameters for Cr 2p region XPS of the spent and fresh catalysts

	Cr 2p3/2 BE (eV)		Cr 2p1/2 BE (eV)	
Catalysts	Cr(VI)	Cr(III)	Cr(VI)	Cr(III)
With H_2O-100 h	—	575.96	586.88	585.90
Without H_2O-8 h	577.02	576.71	—	586.69
Fresh catalyst	577.56	577.13	588.17	586.77
With H_2O-30 h	578.47	576.87	586.97	586.69

complexity of Cr(III), it is quite hard to ascertain the contribution of the intermediate chromium state in the Cr 2p3/2 region. Studies have shown that both Cr(VI) and Cr(III) are the catalytic activity centres of ODH; however, Cr(VI) is usually unstable and easily reduced.[25] It can be observed that the fresh catalyst and the catalyst with H_2O-30 h mainly appear at the binding energies of Cr(III) at 577.08 eV and 577.28 eV (2p3/2).[37,38] At the same time, the catalysts without H_2O-8 h and with H_2O-100 h displayed Cr (close to a zero-valent state) at the binding energies of 576.88 eV and 576.28 eV. The relative amount of Cr(III) increased in the used sample compared with a fresh catalyst, indicating the reduction of Cr(VI) to Cr(III), and the result is in agreement with the conclusions reported in the recent literature.[15,39] The binding energy of Cr(III) decreased with increasing reaction time; meanwhile, a close to zero-valent state of Cr generally formed, leading to the decrease in the catalytic activity on the catalyst surface, and eventually the catalytic performance dropped. Furthermore, the decrease in interaction between adsorbed oxygen and the active component is probably due to the adsorption of water molecules on the active component surface. Therefore, the addition of water vapour is beneficial to inhibit carbon deposition and deep oxidation on the catalyst surface. Because coke formation is the main factor of the deactivation process of ODH, we characterized the basic coke information of the catalyst before and after catalytic reaction. Fig. 12 shows the XPS of C1s of the fresh catalyst and spent 18% Cr/ZnAlLaO catalysts. One main peak and some broad peaks are observed in each case. The area percentages and quantitative data of binding energies are summarized in Table 2. The C1s region spectra display the features corresponding to the various chemical nature of carbon: pregraphite-like, aromatic, aliphatic, and partially oxidized, and the binding energies were identified according to the previous reports.[9] As for the fresh catalyst, two main peaks at binding energies of 284.88 and 288.76 eV are detected, which are assigned to the adventitious hydrocarbon (C–C/C–H) and oxidized carbon species (O–C═O), respectively. These are probably from residues after the calcination of the synthesized catalyst or the interaction of the feed gas on the catalyst surface. The value of C–C/C–H is generally shifted toward the lower binding energy with increasing reaction time. In contrast, the C1s spectrum also displays the asymmetric peak shape on the used catalysts (without H_2O-8 h and with H_2O-100 h) at binding energies of 284.28 eV and 283.88 eV. It is obvious that the catalyst with H_2O-100 h achieves the maximum peak intensity (with a binding energy of 283.88 eV), and the coke deposits are possibly composed of the sp^2 hybridized carbon; this type of coke probably consists of aromatic rings according to the previous studies.[40–42] Furthermore, the produced coke deposits of used catalysts without H_2O-8 h and with H_2O-100 h are assigned to the pregraphite-like carbon, which was present in the study.[43] It has a lower binding energy than the graphitic carbon, suggesting a high electron density related to its structure.[42] Moreover, compared to the catalyst without H_2O-8 h, the coke deposit of the pregraphite-like carbon has not been determined in the catalyst with H_2O-30 h, which suggests that the presence of water vapour can decrease the amount of coke on the catalyst surface and improve the stability of ODH reaction. It has also been proven by the consequence of catalytic performance shown in Fig. 11 and 12. The C1s spectrum of the catalyst with H_2O-30 h is similar to that of the fresh catalyst. However, the main peak at 283.88 eV in the catalyst with

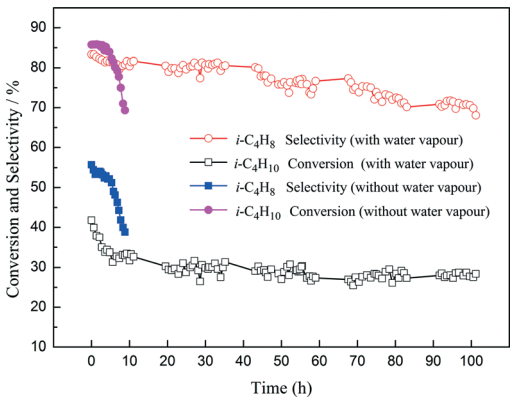

Fig. 11 100 h test comparison of the Cr (18%)/ZnAlLaO catalyst with and without water vapour. Reaction conditions: temperature = 580 °C, 1 atm, 2 g of catalysts, i-C_4H_{10}/O_2 = 3.5 (molar ratio), SV = 200 mL g^{-1} h^{-1}.

Table 2 Curve-fitting parameters for C1s XPS of the spent and fresh catalysts

	C1s BE (eV)				
Catalysts	Pregraphite-like	C–C/C–H	C_xH_y	–C═O	O–C═O
With H_2O-100 h					
BE (eV)	283.88	—	—	287.38	—
Area (%)	84.05	—	—	0.33	—
Without H_2O-8 h					
BE (eV)	284.28	—	285.88	—	—
Area (%)	19.80	—	0.02	—	—
Fresh					
BE (eV)	—	284.88	—	—	288.76
Area (%)	—	77.67	—	—	5.07
With H_2O-30 h					
BE (eV)	—	284.68	—	—	288.88
Area (%)	—	68.18	—	—	3.25

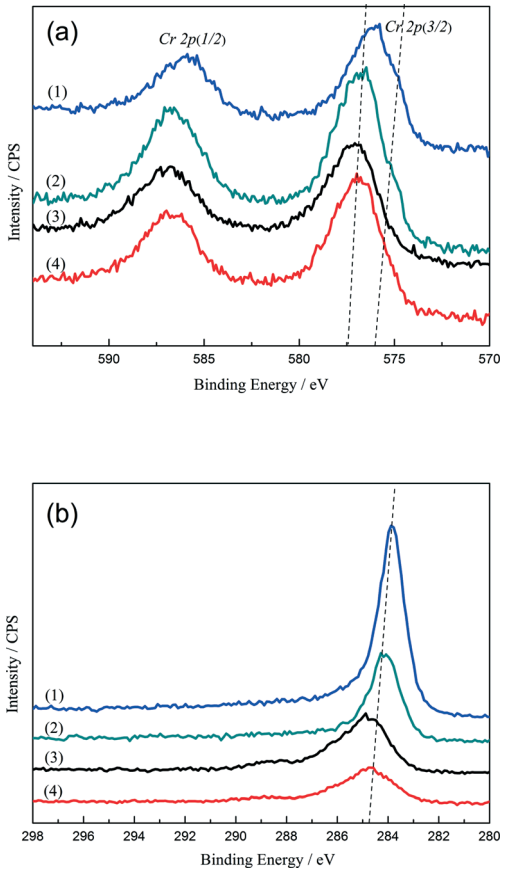

Fig. 12 (a) XPS spectra of chrome over various catalyst surfaces, (b) XPS spectra of carbon over various catalyst surfaces. (1) Cr (18%)/ZnAlLaO catalyst after 100 h test with water vapour (with H_2O-100 h), (2) Cr (18%)/ZnAlLaO catalyst after 8 h test without water vapour (without H_2O-8 h), (3) Cr (18%)/ZnAlLaO fresh catalyst (fresh catalyst), and (4) Cr (18%)/ZnAlLaO catalyst after 30 h test with water vapour (with H_2O-30 h).

H_2O-100 h has a lower binding energy than that of the C1s spectra in the catalyst without H_2O-30 h. This indicates that the coke structure formed over the catalyst with H_2O-100 h has a higher electron density than that over the catalyst without H_2O-30 h.

Apparently, the coke deposit was an important factor for the activity and stability of catalysts. The possible regeneration routes of the catalysts were reported in the literature[33,44] in which several sequential regeneration cycles of various catalysts can be carried out through the method of burning the formed coke[38] under some controlled conditions. For instance, the temperature of the reactor is cooled to about 250 °C, simultaneously using an inert steam such as Ar as the only feeding gas. After reaching this temperature, the inert Ar steam was replaced by an air flow, and then the temperature generally increased to about 550 °C. During this process, the coke formed on the surface of the catalyst was burned through interaction with oxygen gas. Approximately 1 h later, the catalysts were cooled to room temperature and maintained that way overnight. By this measure, the samples were ready to be used in a new cycle.

Optimization of reaction temperature

Fig. 13 shows the catalytic activities of C_4H_{10} and C_4H_8 under various temperatures. It can be seen that the catalytic activity and isobutane conversion are relatively low at temperatures between 560 °C and 570 °C. As the reaction temperature increases, the conversion rate significantly increases. The isobutene selectivity reaches the maximum and stabilizes at about 85% between 570 °C and 585 °C. As the reaction time is prolonged, both the conversion and the selectivity generally decreased. When the temperature becomes too high (600 °C), not only the cracking reaction rate and coke deposition increase but also the catalyst's specific surface area and the active catalysts decrease.[45,46] As shown in Fig. 14, as the temperature increases, cracking reaction generally occurs, which results in the increase in selectivity of CH_4 and C_3H_6 and the decrease in selectivity of CO_2. Hence, the optimal reaction temperature is in the range of 575 °C to 580 °C. The optimal temperature of the fixed bed is in the range of 580 °C to 590 °C. The conversion of isobutane (52.44%) and selectivity of isobutene (84.07%) achieve the optimum at 577 °C.

Optimization of alkoxy oxygen ratio

Table 3 shows the Cr/ZnAlLaO catalytic performances of different alkane oxygen ratios. It can be observed that the isobutene selectivity achieves the maximum when alkoxy ratio is 3.5. When alkoxy ratio is relatively low (ranging from 1 to 3), the intermediates and products are easily converted to by-products such as C_3H_6, CH_4 and CO_2 in the oxygen-enriched environment. In addition, the oxygen-enriched environment can bring competitive adsorption of isobutane to a disadvantageous situation. It leads to the decrease in selectivity of isobutene and the raw material waste. As the alkoxy ratio increases to 3.5, the catalytic activity reaches maximum. When the isobutane content is increased, it can be seen that

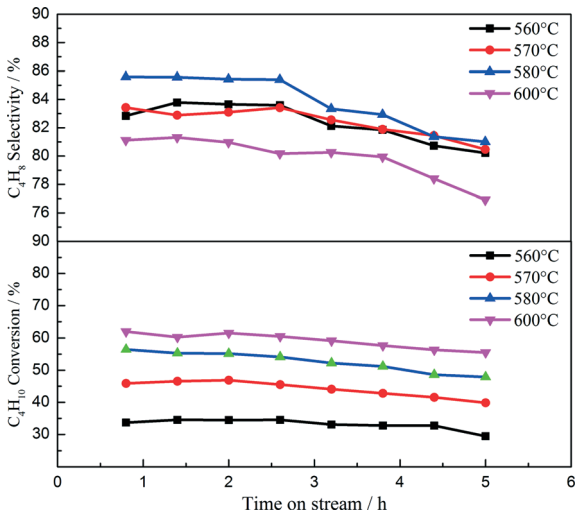

Fig. 13 The C_4H_{10} conversion and C_4H_8 selectivity at different temperatures. Reaction conditions: 1 atm, 2 g of catalysts, i-C_4H_{10}/O_2 = 3.5 (molar ratio), SV = 200 mL g^{-1} h^{-1}, without water vapour.

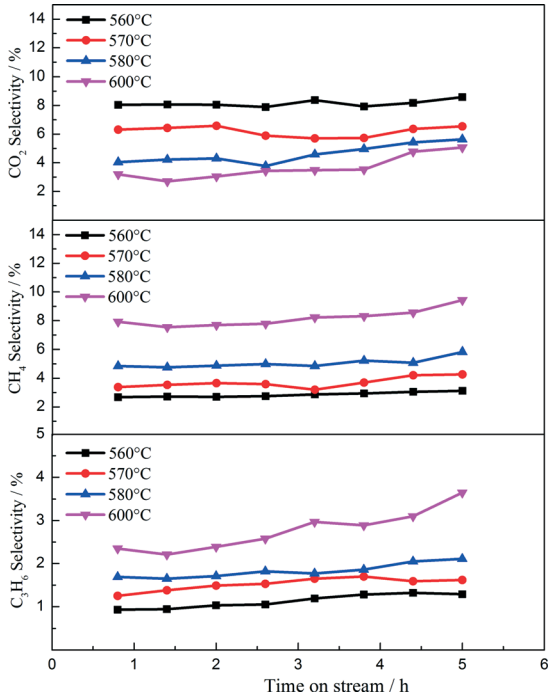

Fig. 14 The selectivity of CH_4, CO_2 and C_3H_6 at different temperatures. Reaction conditions: 1 atm, 2 g of catalysts, i-C_4H_{10}/O_2 = 3.5 (molar ratio), SV = 200 mL g^{-1} h^{-1}, without water vapour.

Table 3 Cr/ZnAlLaO catalytic performance as a function of the alkane/oxygen ratio[a]

	Conversion (%)	Selectivity (%)				
i-C_4H_{10}/O_2	i-C_4H_{10}	i-C_4H_8	C_3H_6	CH_4	CO	CO_2
1.0	43.72	63.71	6.00	8.43	3.78	13.99
2.0	46.27	72.41	5.82	6.03	4.55	7.22
3.0	52.79	80.89	3.45	5.45	3.96	4.17
3.5	52.44	84.07	3.37	4.31	3.53	3.27
4.0	57.04	83.05	3.12	4.56	3.03	2.98
5.0	60.39	72.49	4.81	8.48	3.89	2.54
6.0	60.39	72.49	4.81	8.48	3.89	2.54

[a] Reaction conditions: temperature = 580 °C, 1 atm, 2 g of catalysts, i-C_4H_{10}/O_2 = 3.5 (molar ratio), SV = 200 mL g^{-1} h^{-1}, without water vapour.

the isobutane conversion increases continuously while both isobutene and CO_2 selectivity decrease due to the formation of oxycarbide in the oxygen-poor environment. A C_4H_{10}/O_2 ratio of 6 causes an increase in side reactions and isobutane cracking. In conclusion, we believe that the optimum alkoxy ratio for isobutane ODH ranges from 3 to 4.

Conclusions

In summary, different supports of chromium-based catalysts have an obvious impact on the catalytic activity of isobutane dehydrogenation. The novel ZnAlLaO support shows the best selectivity of isobutene and conversion of isobutene compared with the other supports. Both the even distribution of the active component Cr_2O_3 and the moderate alkalinity over the ZnAlLaO catalyst surface are beneficial for the activity and stability of the catalyst. The addition of an appropriate amount of water vapour as part of the feed gas can effectively inhibit carbon deposition on the catalyst surface and enhance the catalytic stability, whereas both the selectivity and the conversion are decreased. In this case, the optimum reaction temperature is in the range of 575 °C to 580 °C. The alkoxy ratio has been chosen in the range of 3 to 4. In the present study, the catalytic activity of the Cr/ZnAlLaO catalyst has obtained a significant improvement in order to compete with commercial catalysts.

Acknowledgements

This work was supported by the key laboratory research of natural gas and light hydrocarbon catalytic conversion of China University of Petroleum (Beijing).

Notes and references

1 S. T. Korhonen, S. M. K. Airaksinen, M. A. Bañares and A. O. I. Krause, Isobutane dehydrogenation on zirconia-, alumina-, and zirconia/alumina-supported chromia catalysts, *Appl. Catal., A*, 2007, **333**, 30–41.
2 K. J. Caspary, H. Gehrke and M. Heinritz-Adrian, *Dehydrogenation of Alkanes, Handbook of Heterogeneous Catalysis*, Wiley-VCH, pp. 3206–3226.
3 B. Y. Jibril, N. O. Elbashir, S. M. Al-Zahrani and A. E. Abasaeed, Oxidative dehydrogenation of isobutane on chromium oxide-based catalyst, *Chem. Eng. Process.*, 2005, **44**, 835–840.
4 B. J. Grzybowska, R. Sloczynski and K. Grabowski, Chromium Oxide/Alumina Catalysts in oxidative dehydrogenation of isobutane, *J. Catal.*, 1998, **18**(6), 698.
5 Y. Sun, T. A. Robson and T. C. Brown, Kinetics of the oxidative dehydrogenation of isobutene over Cr_2O_3/$La_2(CO_3)_3$, *J. Nat. Gas Chem.*, 2002, **11**, 70–78.
6 P. Moriceau, B. Grzybowska, Y. Barbaux, G. Wrobel and G. Hecquet, Oxidative dehydrogenation of isobutane on Cr–Ce–O oxide, *Appl. Catal., A*, 1998, **168**, 269.
7 W. Grunert, W. Saffert, R. Feldhaus and K. Anders, Reduction and aromatization of chromia-alumina catalysts I. Reduction and break-in behavior of a potassium-promoted chromia-alumina catalyst, *J. Catal.*, 1986, **99**, 149–158.
8 G. B. McVicker, G. M. Kramer and J. J. Ziemia, On the question of carbonium ions as intermediates over silica-alumina and acidic zeolites, *Catal. Today*, 1983, **83**(23), 286–291.
9 J. Silvestre-Albero, J. C. Serrano-Ruiz, A. Sepúlveda Escribano and F. Rodríguez-Reinoso, Modification of the catalytic behaviour of platinum by zinc in crotonaldehyde hydrogenation and iso-butane dehydrogenation, *Appl. Catal., A*, 2005, **292**, 244–251.
10 E. Cornelius and S. H. Milliken, *Dehydrogenation catalyst, US Patent*, 2,956,030.
11 M. P. Atkins and G. R. Evans, Catalytic dehydrogenation-a review of current process and innovations, *Appl. Catal.*, 1995, **46**(2), 271.

12 B. Liu, Y. Fang and M. Terano, *J. Mol. Catal. A: Chem.*, 2004, **219**, 165–173.
13 A. B. Gaspar, C. A. C. Perez and L. C. Dieguez, Characterization of Cr/SiO2 catalysts and ethylene polymerization by XPS, *Appl. Surf. Sci.*, 2005, **252**, 939–949.
14 S. Udomsak and R. G. Anthony, Isobutane dehydrogenation on chromia/silica-titania mixed oxide and chromia/ç-alumina catalysts, *Ind. Eng. Chem. Res.*, 1996, **35**, 47–53.
15 F. Cavani, M. Koutyrev and F. Trifiro, *et al.* Chemical and physical characterization of alumina-supported chromia-based catalysts and their activity in dehydrogenation of isobutane, *Catalysis*, 1996, **158**(24), 236–250.
16 P. Sun, G. Siddiqi, M. Chi and A. T. Bel, Synthesis and characterization of a new catalyst Pt/Mg(Ga)(Al)O for alkane dehydrogenation, *J. Catal.*, 2010, **274**, 192–199.
17 N. O. Elbashir, S. M. Al-Zahrani and A. E. Abasaeed, *et al.* Alumina-supported Chromium-based mixed-oxide catalysts in oxidative dehydrogenation of isobutene to isobutene, *Chem. Eng. Process.*, 2003, **42**, 817–823.
18 S. M. Al-Zahrani, N. O. Elbashir and A. E. Abasaeed, *et al.* Catalytic performance of chromium oxide supported on Al_2O_3 in oxidative dehydrogenation of isobutane to isobutene, *Ind. Eng. Chem. Res.*, 2001, **40**(8), 781–784.
19 M. Hoang, J. F. Mathews and K. C. Pratt, Oxidative dehydrogenation of isobutane over supported chromium oxide on lanthanum carbonate, *J. Catal.*, 1997, **171**(1), 320–324.
20 R. D. Cortright, J. M. Hill and A. Dumesic, Selective dehydrogenation of isobutane over supported Pt/Sn catalysts, *Catal. Today*, 2000, **55**(3), 212–223.
21 B. Grzybowska, J. Sloezynaloi and R. Gratowzki, *et al.* Oxidation of C_2–C_4 alkanes on chromium oxide/alumina and Don Cr_2O_3: Catalytic and TPD Studies, *Appl. Catal., A*, 2001, **209**(1/2), 279–289.
22 A. Miyamoto and Y. Murakami, Determination of the number of active oxygen species on the surface of Cr_2O_3 catalysts, *Catal. Today*, 1983, **80**(6), 106.
23 B. M. Weckhuysen, L. M. Ridder and P. Grobet, *et al.* Redox behavior and dispersion of supported chromium catalysts, *J. Phys. Chem.*, 1995, **99**(1), 320–326.
24 S. Debaprasad and S. Abdelhamid, Light alkane dehydrogenation over mesoporous Cr_2O_3/Al_2O_3 catalysts, *Appl. Catal., A*, 2010, **389**, 155–164.
25 L. W. Lin, W. S. Yang, J. F. Jia, Z. S. Xu, T. Zhang, Y. N. Fan, Y. Kou and J. Y. Shen, Surface structure and reaction performances of highly dispersed and supported bimetallic catalysts, *Sci. China, Ser. B: Chem.*, 1999, **42**, 571–580.
26 M. Cherian, M. S. Rao, A. M. Hirt, I. E. Wachs and G. Deo, Oxidative dehydrogenation of propane over supported chromia catalysts: Influence of Oxide Supports and Chromia Loading, *J. Catal.*, 2002, **211**, 482–495.
27 Y. Zhang, Y. Zhou, L. Wan, M. Xue, Y. Duan and X. Liu, Effect of magnesium addition on catalytic performance of PtSnK/γ-Al_2O_3 catalyst for isobutane dehydrogenation, *Fuel Process. Technol.*, 2011, **92**, 1632–1638.
28 M. Guisnet and N. S. Gnep, Aromatization of propane over Ga HMFI catalysts. Reaction scheme, nature of the dehydrogenation species and mode of coke formation, *Catal. Today*, 1996, **31**, 275–292.
29 L. W. Lin, T. Zhang, J. L. Zang and Z. S. Xu, Dynamic process of carbon deposition on Pt and Pt–Sn catalysts for alkane dehydrogenation, *Appl. Catal.*, 1990, **67**, 11–23.
30 S. De Rossi, M. P. Casaletto, G. Ferraris, A. Cimino and G. Minelli, Chromia/zirconia catalysts with Cr content exceeding the monolayer. A comparison with chromia/alumina and chromia/silica for isobutane dehydrogenation, *Appl. Catal., A*, 1998, **167**, 257–270.
31 M. Ohta, Y. Ikeda and A. Igarashi, Additive effect of Sn in Pt–Sn/ZnO–Cr_2O_3 catalyst for low-temperature dehydrogenation of isobutane, *Appl. Catal., A*, 2004, **266**, 229–233.
32 G. Siddiqi, P. Sun, V. Galvita and A. T. Bell, Catalyst performance of novel Pt/Mg(Ga)(Al)O catalysts for alkane dehydrogenation, *J. Catal.*, 2010, **274**, 200–206.
33 D. Duprez and J. Barbier, Effect of stream on the coking and on the regeneration of metal catalysts: a comparative study of alumina-supported platinum, rhenium, iridium and rhodium catalysts, *Stud. Surf. Sci. Catal.*, 1991, **68**(3), 111–117.
34 B. J. Liaw, D. S. Cheng and B. L. Yang, Oxidative Dehydrogenation of Isobutene on iron oxyhydroxides and hydrated iron oxides, *Appl. Catal.*, 1989, **118**(3), 312.
35 L. Mikael, H. Magnus, A. B. Edd and A. Bengt, The effect of reaction conditions and time on stream on the coke formed during propane dehydrogenation, *J. Catal.*, 1996, **164**, 44–53.
36 I. Ikemoto, K. Ishi, S. Kinoshita and H. Kuroda, *et al.* Chromium(III) hydroxide oxide, *J. Solid State Chem.*, 1976, **17**, 425.
37 B. Liu and M. Terano, Investigation of the Physico-Chemical State and Mechanism of Surface Cr Species on a Phillips CrO_x/SiO_2 Catalyst by XPS, *Catalysis*, 2001, **172**(6), 227.
38 G. J. Siri, J. M. Ramallo-López, M. L. Casella, J. L. G. Fierro, F. G. Requejo and O. A. Ferrettia, XPS and EXAFS study of supported PtSn catalysts obtained by surface organometallic chemistry on metals application to the isobutane dehydrogenation, *Appl. Catal., A*, 2005, **278**, 239–249.
39 J. Słoczyński, B. Grzybowska, R. Grabowski, A. Kozłowska and K. Wcisio, Oxygen adsorption and catalytic performance in oxidative dehydrogenation of isobutane on chromium oxide-based catalysts, *Phys. Chem. Chem. Phys.*, 1999, **1**, 333–339.
40 E. Desimoni, G. I. Casella, A. Morone and A. M. Salvi, XPS determination of oxygen-containing functional groups on carbon-fibre surfaces and the cleaning of these surfaces, *Surf. Interface Anal.*, 1990, **15**, 627.
41 M. G. Cutrufello, S. De Rossi, I. Ferino, R. Monaci, E. Rombi and V. Solinas, Preparation, characterisation and activity of chromia–zirconia catalysts for propane dehydrogenation, *Thermochim. Acta*, 2005, **434**, 62–68.
42 B. K. Vu, M. B. Song, S.-A. Park, Y. Lee and I. Y. Ahn, Electronic density enrichment of Pt catalysts by coke in the propane dehydrogenation, *Korean J. Chem. Eng.*, 2011, **28**(2), 383–387.

43 B. K. Vu, S. Bok, I. Y. Ahn and E. W. Shin, Oxidation of Coke Formed Over Pt-Al_2O_3 and Pt-SBA-15 in Propane Dehydrogenation, *Catal. Lett.*, 2009, **133**, 376.

44 S. M. Stagg, C. A. Querini, W. E. Alvarez and D. E. Resasco, Isobutane Dehydrogenation on Pt–Sn/SiO_2 Catalysts: Effect of Preparation Variables and Regeneration Treatments, *J. Catal.*, 1997, **168**, 75.

45 V. Z. Fridman, Pathways of light compounds formation during propane and isobutene dehydrogenation on Al-Cr catalysts, *Appl. Catal., A*, 2010, **382**, 139–147.

46 N. A. Pakhomova, V. N. Kashkina, E. I. Nemykina, V. V. Molchanov, V. I. Nadtochiy and A. S. Noskov, Dehydrogenation of C_3–C_4 paraffins on Cr_2O_3/Al_2O_3 catalysts in fluidized and fixed bed reactors, *Chem. Eng. J.*, 2009, **154**, 185–188.